

# Three Distinct Solvated Structures of *p*-Nitroaniline in Acetonitrile/ $\text{CCl}_4$ Mixed Solvents: A Combined Singular Value Decomposition Analysis of Ultraviolet Absorption and Raman Spectra

Kathaperumal Mohanalingam, Daisuke Yokoyama,<sup>†</sup> Chihiro Kato,<sup>††</sup> and Hiro-o Hamaguchi<sup>\*,†</sup>

Advanced Research Center for Science and Engineering, Waseda University, Okubo, Shinjuku-ku, Tokyo 169-8555

<sup>†</sup>Department of Chemistry, School of Science, The University of Tokyo, Hongo, Bunkyo-ku, Tokyo 113-0033

<sup>††</sup>Basic Technology Division, Kanagawa Industrial Technology Research Institute, Ebina 243-0435

(Received November 12, 1998)

Ultraviolet absorption and Raman spectra of *p*-nitroaniline (pNA) have been measured in acetonitrile/ $\text{CCl}_4$  mixed solvents for seventeen different fractions of acetonitrile. The observed spectral changes were interpreted with the use of a combined singular value decomposition (SVD) analysis, in which the ultraviolet absorption and Raman spectra were combined into one set of spectra. A least-squares fitting analysis was carried out for the SVD decomposed spectra and their amplitudes, using a model in which three distinct species of pNA, the 1:0, 1:1, and 1:2 species, exist in equilibrium. Here, the 1:0, 1:1, and 1:2 species have 0, 1, and 2 acetonitrile molecules associated with pNA. Three intrinsic ultraviolet absorption and Raman spectra have been obtained as a result of the fitting analyses. The three intrinsic spectra show different degrees of charge transfer in the three different solvated forms of pNA. Two equilibrium constants,  $K_1$  for the equilibrium between the 1:0 and 1:1 species and  $K_2$  for 1:1 and 1:2, have been determined. These equilibrium constants give the standard free energy changes for the association of acetonitrile with pNA. A microscopic and quantitative view on the solvation of pNA in acetonitrile/ $\text{CCl}_4$  mixed solvents has thus been established.

Molecules having electron donor and acceptor end groups separated by a conjugated backbone are of considerable interest because they serve as excellent models for studying the mechanism of intra- and intermolecular charge-transfer (CT) processes.<sup>1–9</sup> They are also practically important for their potentiality as nonlinear optical materials.<sup>10,11</sup> One of the simplest molecules of this type, *p*-nitroaniline (hereafter pNA), has an electron-donating amino group and an electron-accepting nitro group connected by a benzene ring. This molecule is well known for its marked solvatochromism;<sup>2–5</sup> the ultraviolet absorption peak of pNA shifts from 329 nm in carbon tetrachloride ( $\text{CCl}_4$ ) to 365 nm in acetonitrile (AN). This large shift of electronic absorption has been interpreted in terms of the CT character of the lowest excited singlet state ( $S_1$ ). In a polar solvent, the  $S_1$  state is more stabilized than in a nonpolar solvent because of its CT character, while the non-CT ground state ( $S_0$ ) is not much affected by the solvent polarity.<sup>9</sup> The  $S_0 \rightarrow S_1$  transition energy therefore becomes lower and hence the absorption peak shifts to the red in a polar solvent. Recently, we carried out a detailed study of this solvatochromism of pNA using AN/ $\text{CCl}_4$  mixed solvents, in which the solvent polarity could be changed continuously by changing the AN fraction.<sup>12</sup> Our original intention was to quantify the polarity of the AN/ $\text{CCl}_4$  mixed solvent from the shift of the pNA electronic absorption. As expected, spectral changes with continuous red peak shift were ob-

served when the AN fraction was increased. However, a singular value decomposition (SVD) analysis<sup>12–22</sup> indicated that these spectral changes should be ascribed to the varying degrees of contributions from three independent basis spectra rather than to a continuous shift of a single absorption band. Based on the SVD result, we came to a conclusion that three distinct forms of pNA exist in AN/ $\text{CCl}_4$  mixed solvents, namely, free pNA (1:0 species) and two associated forms of pNA (1:1 species and 1:2 species). The 1:1 species has one AN molecule associated with pNA and the 1:2 species has two AN molecules associated. In neat  $\text{CCl}_4$ , only the 1:0 species exist. As the AN fraction increases, the number of the 1:1 species grows first and then the 1:2 species becomes dominant. In pure AN, only the 1:1 and 1:2 species exist, with an approximate ratio of 1:4. The three species each has its own intrinsic absorption spectrum whose absorption maximum shifts to the red with increasing number of AN associated with pNA species. The observed continuous spectral changes are attributed to the change of the equilibrium among the three distinct forms of pNA. Thus, the peak shift of the pNA absorption does not give a simple measure of the polarity of the AN/ $\text{CCl}_4$  mixture. The solute/solvent interaction in the pNA/AN/ $\text{CCl}_4$  system seems to be more specific than the aforementioned CT mechanism, which takes the effect of the solvent simply as polarity. In other words, the pNA/AN/ $\text{CCl}_4$  system provides a unique

opportunity for studying the so-called "solvent effect" from the viewpoint of specific intermolecular interactions between the solute and the solvent molecules.

In order to obtain further insight into the interaction of pNA with AN, we studied the Raman spectra of pNA in the same AN/CCl<sub>4</sub> mixed solvents.<sup>23)</sup> We found that both the NH<sub>2</sub> symmetric stretch frequency of the amino group and the NO<sub>2</sub> symmetric stretch frequency of the nitro group showed marked downshifts with increasing the AN fraction. From the magnitude of the observed downshifts in these vibrational frequencies, we were able to conjecture the structure of the two associated forms of pNA; one AN molecule is attached to the amino part of pNA in the 1 : 1 species and two molecules are attached, one to the amino part and the other to the nitro part, in the 1 : 2 species.

In the present paper, we report a combined SVD analysis of the ultraviolet absorption and the Raman spectra of pNA in AN/CCl<sub>4</sub>. The present analysis is more quantitative than previous ones in two ways. 1) Using the same concentration of pNA ( $5 \times 10^{-4}$  mol dm<sup>-3</sup>) for both the ultraviolet absorption and Raman spectral measurements, we are able to carry out the SVD fitting analysis (see the following section of SVD analysis) using model functions that are common to the ultraviolet absorption and Raman spectral changes. We note here that the concentration  $5 \times 10^{-4}$  mol dm<sup>-3</sup> is too low for ordinary Raman spectral measurements. We therefore used near ultraviolet excitation at 413.5 nm so that Raman cross sections could be increased by the pre-resonance effect.<sup>24)</sup> It was found that the pre-resonance effect was large enough for the NO<sub>2</sub> symmetric stretch band, but not for the NH<sub>2</sub> symmetric stretch band. Therefore, the NH<sub>2</sub> symmetric stretch band is not included in the present analysis. 2) The AN fraction dependence of each of the three species is modeled on the basis of the law of mass action. The use of the law of mass action leads to the estimation of the two equilibrium constants  $K_1$  and  $K_2$ , where  $K_1$  is for the equilibrium between the 1 : 0 and 1 : 1 species and  $K_2$  for 1 : 1 and 1 : 2. Thus the present combined SVD analysis not only confirms further the existence of the three distinct forms of pNA in AN/CCl<sub>4</sub> mixed solvents but also gives quantitative information on the nature of the association between pNA and AN molecules.

### Experimental

The sample of pNA was commercially obtained from Wako Pure Chemicals Co. and was purified by vacuum sublimation. HPLC grade acetonitrile and carbon tetrachloride were purchased from Wako Chemicals Co. and used as received. The concentration of pNA was  $5 \times 10^{-4}$  mol dm<sup>-3</sup> for both the ultraviolet absorption and Raman spectral measurements. Seventeen different mixed solvents containing 0, 0.5, 1.0, 1.5, 2.0, 2.5, 3.0, 4.0, 5.0, 10.0, 15.0, 20.0, 30.0, 40.0, 60.0, 80.0, and 100 volume % of AN were prepared and used for the spectral measurements. These volume % values correspond to AN molar fractions of 0,  $9.26 \times 10^{-3}$ ,  $1.84 \times 10^{-2}$ ,  $2.75 \times 10^{-2}$ ,  $3.66 \times 10^{-2}$ ,  $4.55 \times 10^{-2}$ ,  $5.44 \times 10^{-2}$ ,  $7.19 \times 10^{-2}$ ,  $8.92 \times 10^{-2}$ ,  $1.71 \times 10^{-1}$ ,  $2.47 \times 10^{-1}$ ,  $3.17 \times 10^{-1}$ ,  $4.43 \times 10^{-1}$ ,  $5.53 \times 10^{-1}$ ,  $7.36 \times 10^{-1}$ ,  $8.81 \times 10^{-1}$ , 1.00.

The ultraviolet absorption spectra were recorded on a Hitachi U-3500 UV-vis absorption spectrophotometer using a 1 mm path

quartz cuvette. The Raman spectra were measured using the 413.1 nm line of a Spectra Physics BeamLok 3200 Kr<sup>+</sup> laser for excitation. Typical laser power used was 35 mW. The sample solutions were sealed in glass cells. The Raman scattered light was collected by a camera lens, dispersed by a single polychromator, and detected by an Astromed CCD 3200 detector.

The observed Raman spectra were normalized by using the 790 cm<sup>-1</sup> band of CCl<sub>4</sub> as the internal standard. Between 0 and 20% AN concentration, a clear linear relation holds between the peak intensity of this standard band and that of the 919 cm<sup>-1</sup> band of AN (Fig. 1). However for higher AN fraction, the observed intensity of the 919 cm<sup>-1</sup> band of AN deviates significantly from the linear relationship. The deviation probably means a nonuniformity of the mixed solvent above 20 volume % of AN; the AN molecules may form domains at higher concentrations. Although this observation is of interest in itself, we do not go into its details. As shown later, we confine our SVD analysis to the range of low AN fraction (less than 20 volume %), so that we treat mixed solvents in which the AN molecules are expected to be dispersed uniformly and hence the concentration and molar fraction of AN can be well defined.

**Singular Value Decomposition Analysis.** Singular value decomposition (SVD) analysis<sup>12–22)</sup> is based on a mathematical theorem that any two dimensional ( $i \times j$ ) matrix  $O$  can be expressed as a product of three matrices  $A$  ( $i \times i$ ),  $W$  ( $i \times i$ ), and  $S$  ( $i \times j$ );  $O = AWS$ . In the present analysis, the matrix  $O$  consists of 12 sets of ultraviolet absorption and Raman spectra measured at 12 different AN molar fractions (0 to 3.17). The ultraviolet and Raman spectra at each AN fraction are combined into one spectrum which has 642 data points, 461 from the ultraviolet absorption spectrum and 181 from the Raman. The relative weight between the ultraviolet and Raman spectra is so determined that they have similar amplitudes as a whole. The  $i$ th row of the matrix  $O$  represents the combined ultraviolet/Raman spectrum at the  $i$ th AN molar fraction ( $i = 1–12$ ). The SVD procedure decomposes  $O$  into 12 spectra  $s_n$  with its amplitude  $a_n$  where  $s_n$  is a row vector having 642 elements and  $a_n$  is a column vector having 12 elements. The spectrum matrix  $S$  is a  $12 \times 642$  matrix whose  $n$ th row is  $s_n$ . The amplitude matrix  $A$  is a  $12 \times 12$  matrix whose  $n$ th column is  $a_n$ . The singular value matrix

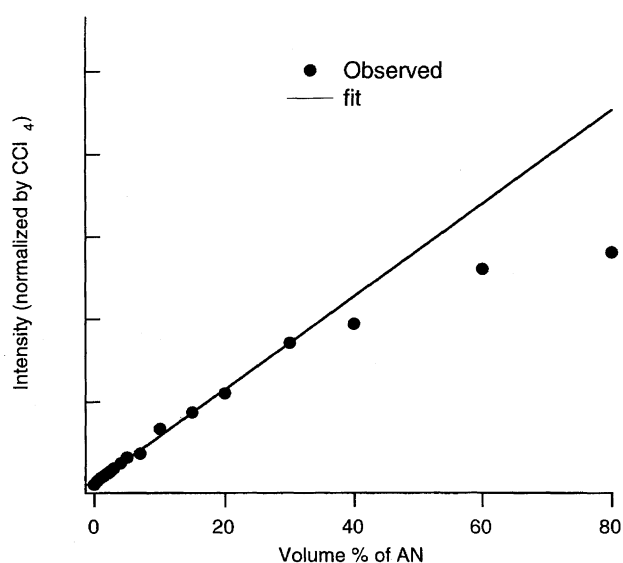
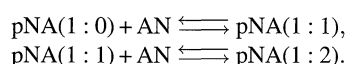


Fig. 1. Normalized Raman intensity of the 919 cm<sup>-1</sup> band of AN versus the volume percent of AN (see text for further details).

$W$  is a  $12 \times 12$  diagonal matrix whose  $(n-n)$ th element is the  $n$ th singular value  $w_n$ . The  $n$ th singular value  $w_n$  represents the weight with which the  $n$ th spectrum  $s_n$  contributes to the observed spectra  $O$ . If there are only  $m$  ( $m < 12$ ) independent spectra involved, we should have  $m$  non-zero singular values and  $(12 - m)$  zero singular values. In reality, however, the distinction of the non-zero and zero singular values is often difficult because of the noise in the observed spectra. As already mentioned in the Introduction and as will be confirmed later, we have three distinct species of pNA that account for the spectral changes represented by the matrix  $O$ . This means that  $m = 3$ . Once the number  $m$  is fixed to three, only three spectra  $s_1$ ,  $s_2$ , and  $s_3$  having the largest three singular values and the corresponding three amplitudes  $a_1$ ,  $a_2$ , and  $a_3$  need to be taken into account. The remaining SVD components with  $n > 3$  are disregarded as noise.

The three spectra and amplitudes are, however, not physically meaningful as they are. SVD is a purely mathematical procedure and no physical constraints are involved in it. Thus, with some physical insight into the origin of the spectral changes, we have to recombine  $s_1$ ,  $s_2$ , and  $s_3$  into three intrinsic spectra  $s'_1$ ,  $s'_2$ , and  $s'_3$  of the 1:0, 1:1, and 1:2 species of pNA. At the same time, the three amplitudes  $a_1$ ,  $a_2$ , and  $a_3$  are recombined into the physically meaningful amplitudes  $a'_1$ ,  $a'_2$ , and  $a'_3$  that represent the AN molar fraction dependence of the number of the three pNA species. In the present analysis, the numbers of the three species normalized to the total number of the pNA molecules are taken as the amplitudes. Note that the total number of the pNA molecules is fixed ( $5 \times 10^{-4}$  mol dm $^{-3}$  in concentration) in the experiment and that the numbers of the three pNA species are proportional to their amplitudes. Then, the amplitude  $a'_m$  ( $m = 1, 2, 3$ ) represents the AN molar fraction dependence of the number of the  $m$ th pNA species. We model this AN molar fraction dependence of the amplitude assuming equilibria among the three pNA species;



We define two equilibrium constants  $K_1$  and  $K_2$  as

$$K_1 = x_{1:1}/(x_{1:0}x_{\text{AN}}), \quad (1)$$

$$K_2 = x_{1:2}/(x_{1:1}x_{\text{AN}}), \quad (2)$$

where  $x$  represents the molar fraction. Equations 1 and 2 hold for all AN fractions ( $i = 1-12$ ). At  $i$ th AN molar fraction  $x_{\text{AN}}^i$ , we can replace the molar fractions  $x_{1:0}^i$ ,  $x_{1:1}^i$ ,  $x_{1:2}^i$ , with their amplitudes  $a_1^i$ ,  $a_2^i$ ,  $a_3^i$ , using the relation  $x_{1:1}^i/x_{1:0}^i = a_2^i/a_1^i$  and  $x_{1:2}^i/x_{1:1}^i = a_3^i/a_2^i$ . Then we can solve Eqs. 1 and 2 under the condition  $a_1^i + a_2^i + a_3^i = 1$  and express three amplitudes in terms of  $x_{\text{AN}}^i$ ,  $K_1$ , and  $K_2$ :

$$a_1^i = 1/(1 + K_1x_{\text{AN}}^i + K_1K_2(x_{\text{AN}}^i)^2), \quad (3)$$

$$a_2^i = K_1x_{\text{AN}}^i/(1 + K_1x_{\text{AN}}^i + K_1K_2(x_{\text{AN}}^i)^2), \quad (4)$$

$$a_3^i = K_1K_2(x_{\text{AN}}^i)^2/(1 + K_1x_{\text{AN}}^i + K_1K_2(x_{\text{AN}}^i)^2). \quad (5)$$

A total set ( $i = 1-12$ ) of Eqs. 3, 4, and 5 gives model functions for  $a'_1$ ,  $a'_2$ , and  $a'_3$ . The three SVD decomposed amplitudes  $a_n$  ( $n = 1, 2, 3$ ) should be expressed as linear combinations of  $a'_1$ ,  $a'_2$ , and  $a'_3$ :

$$a_n = c_{n1}a'_1 + c_{n2}a'_2 + c_{n3}a'_3, \quad (6)$$

where  $c_{nm}$  ( $m = 1, 2, 3$ ) is the coefficient representing the contribution of  $a'_m$  to the  $n$ -th SVD decomposed amplitudes. A least-squares fitting analysis is then used to determine the coefficient  $c_{nm}$

and the equilibrium constants  $K_1$  and  $K_2$  that account for the observed spectral changes most satisfactorily. The same coefficients  $c_{nm}$  also transform  $s_1$ ,  $s_2$ , and  $s_3$  to  $s'_1$ ,  $s'_2$ , and  $s'_3$ :

$$s'_n = c_{1n}s_1 + c_{2n}s_2 + c_{3n}s_3. \quad (7)$$

Thus, once  $c_{nm}$ s are determined by the least-squares fitting, we are able to transform  $s_1$ ,  $s_2$ , and  $s_3$  to  $s'_1$ ,  $s'_2$ ,  $s'_3$  to obtain the intrinsic spectra of the three species of pNA. Finally, the matrix  $O$  can be written as the product of  $A'$  and  $S'$ ,

$$O = A'S', \quad (8)$$

where  $A'$  consists of column vectors  $a'_n$  and  $S'$  consists of row vectors  $s'_n$ . The observed spectral changes are decomposed into three components representing the three species of pNA, each of which has the spectrum  $s'_m$  and the amplitude  $a'_m$  that shows the AN concentration dependence following Eqs. 3, 4, and 5.

## Results and Discussion

### Ultraviolet Absorption and Raman Spectral Features.

Representative ultraviolet absorption and Raman spectra of pNA in AN/CCl $_4$  mixed solvents are shown in Fig. 2 for seven different AN molar fractions. As the AN fraction increases, the ultraviolet absorption spectrum shows a marked bathochromic shift (Fig. 2a). The absorption peak changes from 329 nm in neat CCl $_4$  (0% AN) to 365 nm in neat AN (100% AN). The shift does not seem to be linear with the AN fraction; addition of only 2% of AN produces a shift of as large as 11 nm. This trend strongly suggests that some specific interactions of AN with pNA are involved in the observed spectral changes. In fact, we showed in our previous communication<sup>12)</sup> that these spectral change are due to the presence of three distinct forms of pNA with different degrees of interaction with pNA, namely, the 1:0, 1:1, and 1:2 species of pNA. The intensity of the absorption also changes with the AN molar fraction. It first decreases on going from neat CCl $_4$  to 2% AN and then increases as the AN fraction is further increased. Such a complicated behavior of the absorption intensity change cannot be explained in terms of the traditional CT model based on the solvent polarity. The absence of an isobestic point indicates that the change is not due to a simple equilibrium between two different species of pNA, either.

The Raman spectra in the 1200–1360 cm $^{-1}$  region show features due to the NO $_2$  symmetric stretch vibrations of pNA (Fig. 2b). As stated in the Experimental section, the Raman intensities are normalized with the use of the 790 cm $^{-1}$  band of CCl $_4$  as the internal standard. However, this normalization procedure is not applicable to the spectrum in neat AN. Therefore, the Raman spectrum for 100% AN should be regarded as a guide to the eye for the relative Raman intensities. The higher wavenumber band in the 1330–1340 cm $^{-1}$  region is ascribed to the 1:0 and 1:1 species which have no AN molecule attached to the NO $_2$  part and the lower wavenumber band around 1315 cm $^{-1}$  to the 1:2 species which has an AN molecule attached. The down-shift of more than 15 cm $^{-1}$  is most likely to be caused by the association of an AN molecule. The Raman spectral changes

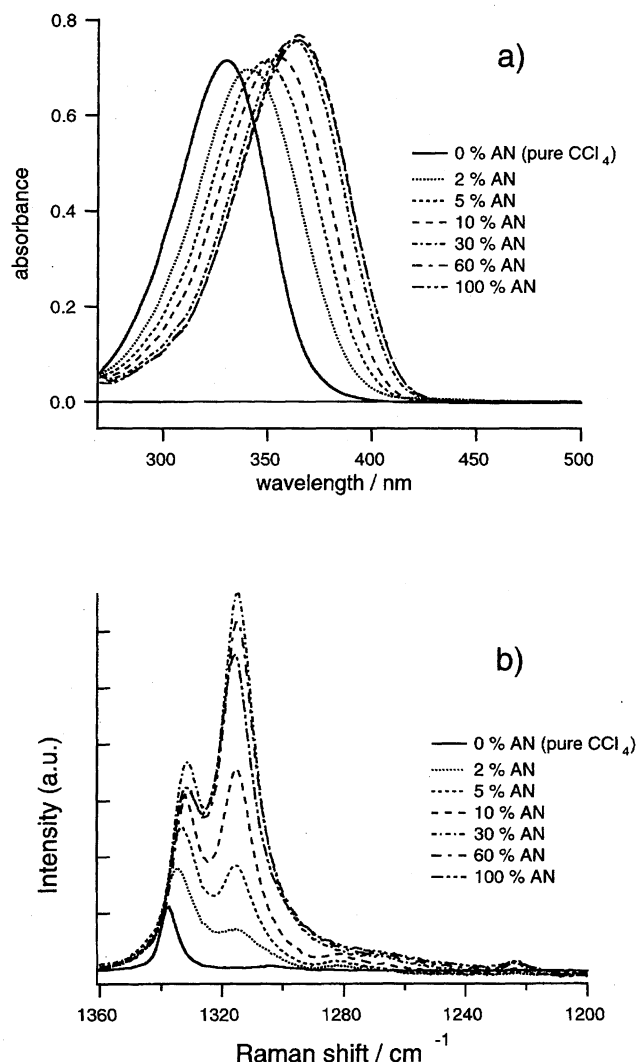


Fig. 2. a) Ultraviolet absorption and b) normalized Raman spectra of pNA in AN/ $\text{CCl}_4$  mixed solvents. The volume percent of AN is given in the figure.

shown in Fig. 2b are very similar to what we have reported earlier,<sup>23)</sup> except for the relative intensities among the three pNA species. This change in relative intensities is a consequence of the pre-resonance effect;<sup>24)</sup> in the present study, the excitation wavelength was 413.1 nm, whereas it was 514.5 nm in the previous experiment.<sup>23)</sup> Thus, the Raman cross section of the 1:2 species, whose absorption maximum is the closest to the exciting line (see below), is more resonance-enhanced than those of the other two species.

**Combined SVD Analysis of the Ultraviolet Absorption and Raman Spectra.** Following the procedures described in the preceding section, we carry out a combined SVD analysis of the ultraviolet absorption and Raman spectral changes as shown in Fig. 2. As stated earlier, 12 AN molar fractions below 0.317 (20 volume%) were used in the analysis. The singular values obtained by SVD are shown in Fig. 3. The magnitudes of the four principal singular values normalized to the largest value are 1, 0.30, 0.07, and 0.01. There is a clear gap between the third and the fourth singular values, in-

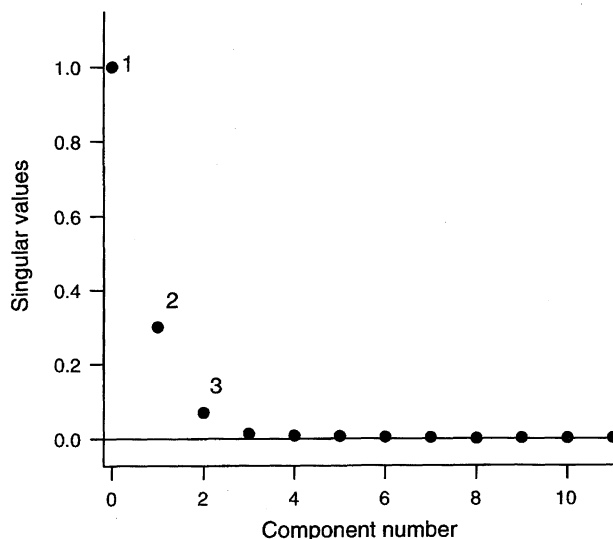


Fig. 3. Singular values obtained from the combined SVD analysis of ultraviolet absorption and Raman spectra of pNA in AN/ $\text{CCl}_4$ .

dicating that the spectral changes in Fig. 2 are actually due to three distinct species. Note here that, if the spectral changes are due to a continuous shift of a single absorption band, SVD should give singular values decreasing continuously without any gap like we see in Fig. 3. The existence of three distinct species, i.e. the 1:0, 1:1, and 1:2 species of pNA, is consistent with our previous results obtained separately for the visible absorption<sup>12)</sup> and Raman spectra.<sup>23)</sup>

We retain the first three SVD components corresponding to the largest three singular values and proceed to a fitting analysis. Figure 4 shows the three SVD amplitudes  $a_1$  (circles),  $a_2$  (triangles),  $a_3$  (squares) as functions of the AN molar fraction. These SVD amplitudes are fitted to model functions given in the form of Eq. 6 using a least-squares method. In

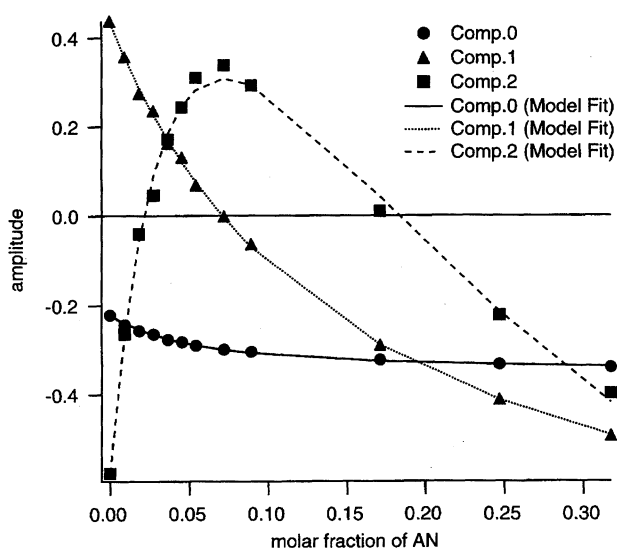


Fig. 4. The AN fraction dependence of the three SVD amplitudes having the largest three singular values from raw SVD analysis. The best fitted curves with Eqs. 3, 4, 5, and 6 are shown together.

doing this least-squares fitting analysis, we assumed that in neat  $\text{CCl}_4$ , only the 1:0 species exists. This is quite a natural assumption, because no AN molecules coexist in neat  $\text{CCl}_4$ . This assumption makes the number of coefficients to be adjusted smaller and makes the least-squares treatment easier. The best fitted model functions thus obtained are shown in Fig. 4 as a full line for  $a_1$ , a dotted line for  $a_2$  and a broken line for  $a_3$ . The SVD-decomposed amplitudes are excellently reproduced with the model functions, indicating that the equilibrium model we use here is physically sound and that the two equilibrium constants  $K_1$  and  $K_2$  thereby determined are meaningful.

Using the coefficients  $c_{nm}$ s obtained from the best fitted functions in Fig. 4, we can convert the three SVD decomposed spectra  $s_1$ ,  $s_2$ , and  $s_3$  to the three intrinsic spectra of the 1:0, 1:1, and 1:2 species of pNA,  $s'_1$ ,  $s'_2$ , and  $s'_3$ . The recomposed spectra are shown in Fig. 5 separately for the ultraviolet absorption (Fig. 5a) and the Raman spectra (Fig. 5b). The spectra of the 1:0 species  $s'_1$  are shown by full lines, those of the 1:1 species  $s'_2$  by dotted lines and those of the 1:2 species  $s'_3$  by broken lines. In the recomposed ultraviolet absorption spectra, the spectrum of the 1:0 species is the same as that observed in neat  $\text{CCl}_4$ . A marked red shift is observed for the 1:1 species and a further red shift is found for the 1:2 species. The absorption maxima and the molar extinction coefficients (in parentheses in the units of  $\text{mol dm}^{-3} \text{ cm}^{-1}$ ) are as follows: 330.5 nm ( $1.4 \times 10^4$ ) for the 1:0 species, 352.5 nm ( $2.0 \times 10^4$ ) for the 1:1 species, 372.5 nm ( $1.6 \times 10^4$ ) for the 1:2 species. Thus, the seemingly continuous shift of ultraviolet absorption of pNA in AN/ $\text{CCl}_4$  mixed solvents (Fig. 2a) is fully ascribed to the three basis spectra (Fig. 5a) contributing differently depending on the AN fraction. The different electronic absorption spectra are indicative of the different CT characters of the three distinct species of pNA.

The recomposed Raman spectra (Fig. 5b) show downshifts of the  $\text{NO}_2$  symmetric stretch frequency with the association of the AN molecule. The peak positions in the recomposed Raman spectra are as follows:  $1337.2 \text{ cm}^{-1}$  for the 1:0 species,  $1333.6 \text{ cm}^{-1}$  for the 1:1 species,  $1314.5 \text{ cm}^{-1}$  for the 1:2 species. These peak positions are very close to those obtained previously by a multi-Lorentzian fitting analysis.<sup>23)</sup> The downshift on going from 1:1 to 1:2 ( $19.1 \text{ cm}^{-1}$ ) is much larger than that on going from 1:0 to 1:1 ( $3.6 \text{ cm}^{-1}$ ). This trend is consistent with our interpretation that the association of AN to the nitro part of pNA takes place on going from the 1:1 species to the 1:2, and not on going from the 1:0 to the 1:1. It is also noted in the Raman spectra in Fig. 5b that the intrinsic intensities are quite different among the three species of pNA. This intensity variance is most likely to be caused by the pre-resonance effect. A marked pre-resonance effect of the  $\text{NO}_2$  symmetric band of pNA has been reported by Schmid et al.<sup>24)</sup> It is thus not surprising if the 1:2 species, whose absorption maximum (372.5 nm) is close to the excitation wavelength (413.1 nm), has much larger Raman cross section than the other two species. The larger Raman intensity of the 1:1 species compared with that

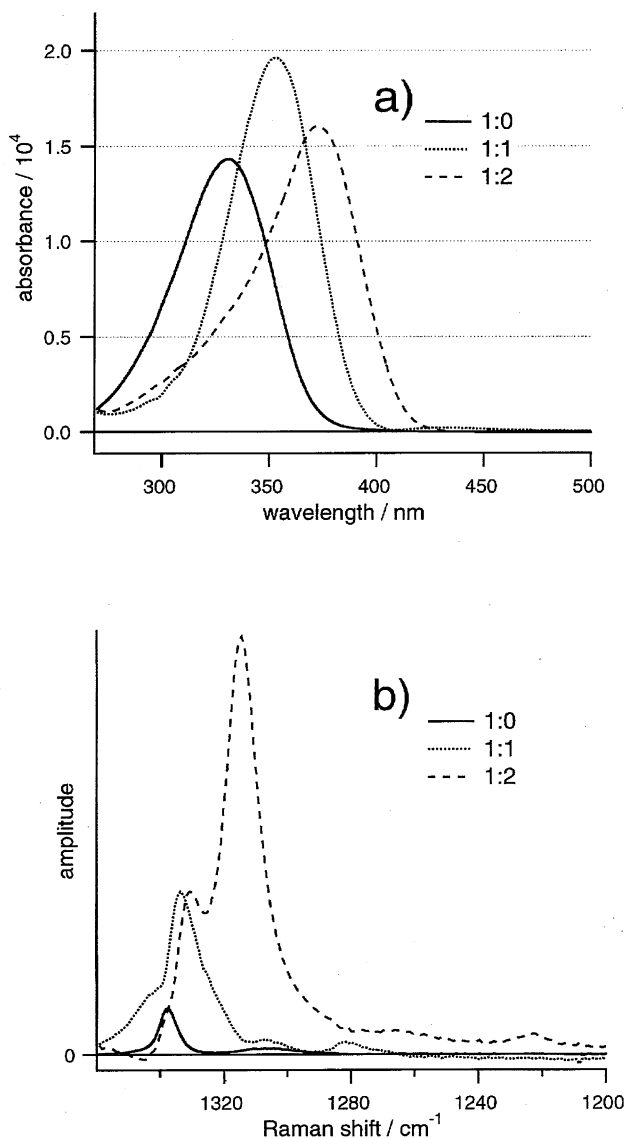


Fig. 5. Result of the combined SVD analysis: a) recomposed ultraviolet absorption and b) Raman spectra of the 1:0, 1:1, and 1:2 forms of pNA.

of 1:0 can also be explained well by the effect of pre-resonance. Another point that should be made here is the fact that the recomposed Raman spectra of the 1:1 and 1:2 species have asymmetric forms. In the case of the 1:2 species, a small shoulder accompanies the principal peak. We believe that these are artifacts due to small continuous downshifts of the intrinsic Raman spectra. In fact, we previously showed by a multi-Lorentzian fitting analysis that the  $\text{NO}_2$  symmetric stretch frequency of each of the three species exhibits a continuous downshift with increasing the AN fraction. This continuous frequency shift is probably due to the change of the dielectric environment of pNA, i.e. the "solvent effect." The SVD analysis cannot take this type of small continuous shift into account.

**Equilibrium among the Three Species of pNA.** The same procedure of the back transformation using the coefficients  $c_{nm}$ s is applied to the SVD amplitudes,  $a_1$ ,  $a_2$ , and  $a_3$ ,

and the AN molar fraction dependence of the amplitudes,  $a'_1$ ,  $a'_2$ , and  $a'_3$  are obtained as shown in Fig. 6. In Fig. 6, filled circles represent  $a'_1$ , triangles represent  $a'_2$  and squares represent  $a'_3$ , respectively. The sum of the amplitudes,  $a'_1 + a'_2 + a'_3$  is shown by open circles. The theoretical curves obtained from Eqs. 3, 4, and 5 with the optimized set of parameters,  $c_{nm}$ s and  $K_1$  and  $K_2$  are also shown in Fig. 6. The agreement between the (SVD recomposed) observed amplitudes and the theoretical curves is excellent. We therefore conclude that the AN molar fraction dependence of the amplitudes of the three pNA species is appropriately represented by the curves in Fig. 6. We note the following three points regarding these curves.

First, the amplitude of the 1:0 species decreases monotonically with increasing the volume% of AN. Even at 0.5 volume% of AN ( $9.26 \times 10^{-3}$  molar fraction), the amplitude of the 1:0 species shows a reduction of about 15% compared with 0% AN, and the 1:1 species shows an increase of a similar magnitude. This trend suggests significant stabilization of the 1:1 species compared with 1:0 when AN molecules are present. Such stabilization of the 1:1 species can be attributed to an increased degree of CT in the pNA chromophore induced by the association of an AN molecule to the amino part. It is likely that the association of AN brings the amino group in plane with the rest of the molecule and thereby promotes the CT from the amino part. Note that pNA takes a nonplanar structure in the crystalline state.<sup>25)</sup> It is well known that the alkylation of one of the amino hydrogens of pNA results in increased CT between the amino and the nitro groups.<sup>4)</sup> This increased CT character is attributed to the increased planarity induced by the alkylation. Second, the amplitude of the 1:1 species increases rapidly with increasing the AN fraction. It reaches a maximum around 5% ( $8.92 \times 10^{-2}$  molar fraction) and then decreases with further increasing the AN fraction. This behavior indicates the ex-

istence of another equilibrium as indicated by Eq. 2. Third, the amplitude of the 1:2 species increases with increasing the AN fraction; after 5%, it keeps increasing at the expense of the 1:0 and 1:1 species. If we extrapolate the curves in Fig. 6 to neat AN (1.00 molar fraction), we obtain the amplitude of 0.003, 0.11, and 0.89 for the 1:0, 1:1, 1:2 species, respectively. These amplitudes are in harmony with our previous estimation that only the 1:1 and 1:2 species exist in the ratio of 1:4 in neat AN.

The two equilibrium constants are determined as  $K_1 = 17.7 \pm 5.2$  and  $K_2 = 4.0 \pm 0.3$ , and the standard free energy changes are also obtained as  $\Delta G_1 = -7.0 \pm 0.7$  kJ mol<sup>-1</sup> and  $\Delta G_2 = -3.4 \pm 0.2$  kJ mol<sup>-1</sup>, respectively. We are now in the process of studying the temperature dependence of the ultraviolet absorption and Raman spectra of the pNA/AN/CCl<sub>4</sub> system, in order to determine the standard enthalpy changes  $\Delta H$ . Combining the  $\Delta G$  and  $\Delta H$  values thus obtained the standard entropy changes  $\Delta S$  can be derived. Then, with all the  $\Delta G$ ,  $\Delta H$ ,  $\Delta S$  values at hand, we will be able to discuss the energetic as well as structural details of the association of AN to pNA in AN/CCl<sub>4</sub> mixed solvents.

### Conclusions

Using the SVD analysis and a kinetic model, we have obtained the intrinsic ultraviolet absorption and Raman spectra of the 1:0 (free form), the 1:1 and the 1:2 associated forms of pNA in AN. The spectra thus obtained illustrate the increasing degree of charge transfer as we go from non-associated (1:0) to the associated (1:2) form. The associated structures are clearly more favored than the nonassociated forms, as it can be evidenced from the equilibrium constants and the standard free energy changes obtained.

The authors are grateful to Dr. Takashi Ogura and Prof. Teizo Kitagawa of Institute for Molecular Science for the 413 nm Raman measurements. Further study of the Raman intensity of the 919 cm<sup>-1</sup> band of AN has shown that the deviation from the straight line in Fig. 1 is primarily due to the change of the band width of the standard band (the 790 cm<sup>-1</sup> band of CCl<sub>4</sub>). If we take the area intensity of the same band as the intensity standard, a good linear relationship has been obtained up to the 80% volume percent of AN.

### References

- 1) M. J. Kamlet, E. G. Kayser, M. E. Jones, J. L. Abboud, J. E. Eastes, and R. W. Taft, *J. Phys. Chem.*, **23**, 2477 (1978).
- 2) T. P. Carsey, G. L. Findley, and S. P. McGlynn, *J. Am. Chem. Soc.*, **101**, 4502 (1979).
- 3) O. S. Khalil, C. J. Selisker, and S. P. McGlynn, *J. Chem. Phys.*, **58**, 1607 (1973).
- 4) R. Nakagaki, I. Aoyama, K. Shimizu, and M. Akagi, *J. Phys. Org. Chem.*, **6**, 261 (1993), and references therein.
- 5) H. K. Sinha and K. Yates, *J. Am. Chem. Soc.*, **113**, 6062 (1991).
- 6) R. W. Bigelow, H. J. Freund, and B. Dick, *Theor. Chim. Acta*, **63**, 177 (1986).
- 7) J. Wolleben and A. C. Testa, *J. Phys. Chem.*, **81**, 429 (1977).

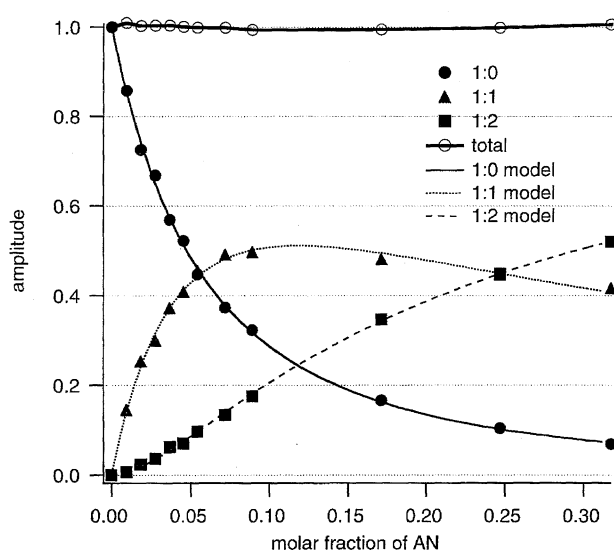


Fig. 6. Recomposed AN fraction dependence of the 1:0, 1:1, and 1:2 forms of pNA. The Sum of the amplitudes of the 1:0, 1:1, and 1:2 forms is also shown as "total" in the figure.

- 8) W. Schuddeboom, J. M. Warman, H. A. Biemans, and E. W. Meijer, *J. Phys. Chem.*, **100**, 12369 (1996).
  - 9) C. Reichardt, "Solvents and Solvent Effects in Organic Chemistry," 2nd ed, VCH, Germany (1988).
  - 10) J. Zyss and D. Chemla, "Nonlinear Optical Properties of Organic Molecules and Crystals," Academic Press, New York (1987).
  - 11) S. R. Mader, J. E. Sohn, and G. D. Stucky, "Materials for Nonlinear Optics: Chemical Perspectives," ACS Symposium. Ser. 455, American Chemical Society, Washington, D.C. (1991).
  - 12) K. Mohanalingam and H. Hamaguchi, *Chem. Lett.*, **1997**, 157.
  - 13) T. Yuzawa and H. Hamaguchi, *J. Mol. Struct.*, **352/353**, 489 (1995).
  - 14) S. Yamaguchi and H. Hamaguchi, *J. Mol. Struct.*, **379**, 87 (1996).
  - 15) S. Yamaguchi, Ph. D. Thesis, The University of Tokyo, Japan, December, 1997.
  - 16) S. Yamaguchi and H. Hamaguchi, *J. Chem. Phys.*, **109**, 1397 (1998).
  - 17) W. G. Chen and M. S. Braiman, *Photochem. Photobiol.*, **54**, 905 (1991).
  - 18) R. Maurer, J. Vogel, and S. Schneider, *Photochem. Photobiol.*, **46**, 247 (1987).
  - 19) S. J. Hug, J. W. Lewis, C. M. Einterz, T. E. Thorgeirsson, and D. S. Kliger, *Biochemistry*, **29**, 1475 (1990).
  - 20) J. Hofrichter, E. R. Henry, J. H. Sommer, R. Deutsch, M. Ikeda-Saito, T. Yonetani, and W. A. Eaton, *Biochemistry*, **24**, 2667 (1985).
  - 21) K. Mohanalingam, S. Yamaguchi, and H. Hamaguchi, *Laser Chem.*, in press.
  - 22) W. H. Press, B. P. Flannery, S. A. Teukolsky, and W. T. Vetterling, "Numerical Recipes in C," Cambridge University Press, Cambridge (1988).
  - 23) K. Mohanalingam and H. Hamaguchi, *Chem. Lett.*, **1997**, 537.
  - 24) E. D. Schmid, M. Moschallski, and W. L. Peticolas, *J. Phys. Chem.*, **90**, 2340 (1986), and references therein.
  - 25) K. N. Trueblood, E. Golgish, and J. Donohue, *Acta Crystallogr.*, **14**, 1009 (1961).
  - 26) K. Mohanalingam and H. Hamaguchi, unpublished result.
-